Resistive switching in polycrystalline $YMnO_3$ thin films

Cite as: AIP Advances **4**, 107135 (2014); https://doi.org/10.1063/1.4899188
Submitted: 13 May 2014 . Accepted: 11 October 2014 . Published Online: 20 October 2014

A. Bogusz, A. D. Müller, D. Blaschke, I. Skorupa, D. Bürger, A. Scholz, O. G. Schmidt, and H. Schmidt

Resistive switching in polycrystalline $YMnO_3$ thin films

A. Bogusz,[1,2,a] A. D. Müller,[3] D. Blaschke,[1,2] I. Skorupa,[1] D. Bürger,[2] A. Scholz,[1] O. G. Schmidt,[2,4] and H. Schmidt[2]
[1]*Institute of Ion-Beam Physics and Materials Research, Helmholtz-Zentrum Dresden-Rossendorf, 01328 Dresden, Germany*
[2]*Chemnitz University of Technology, 09107 Chemnitz, Germany*
[3]*Anfatec Instruments AG, 08606 Oelsnitz, Germany*
[4]*Institute for Integrative Nanosciences, IFW Dresden, 01069 Dresden, Germany*

(Received 13 May 2014; accepted 11 October 2014; published online 20 October 2014)

We report a unipolar, nonvolatile resistive switching in polycrystalline $YMnO_3$ thin films grown by pulsed laser deposition and sandwiched between Au top and Ti/Pt bottom electrodes. The ratio of the resistance in the OFF and ON state is larger than 10^3. The observed phenomena can be attributed to the formation and rupture of conductive filaments within the multiferroic $YMnO_3$ film. The generation of conductive paths under applied electric field is discussed in terms of the presence of grain boundaries and charged domain walls inherently formed in hexagonal $YMnO_3$. Our findings suggest that engineering of the ferroelectric domains might be a promising route for designing and fabrication of novel resistive switching devices. [http://dx.doi.org/10.1063/1.4899188]

I. INTRODUCTION

The continuous search for even smaller and more power-efficient devices, preferably with additional novel functionalities has greatly influenced the research in materials science and the physics of electronics. Resistive switching in insulators and semiconductors is an example of intensively investigated nanoscale phenomena over the last decade. It refers to the nanoscale, nonvolatile resistance change phenomena in a thin films sandwiched by two electrodes by applying current or voltage.[1,2] Such devices could lead to novel implementations of memory and logic devices and contribute to the development of artificial neural network systems.[3] Another fascinating nanoscale phenomenon of recent focus is closely related to the nature of ferroelectric domain walls (DWs). DWs, existing naturally in ferro- and multiferroics, are formed as a result of minimizing the depolarization energy. They can be regarded as structures of reduced dimensionality and their properties can differ substantially from those of the parent material.[4,5] Multiferroic $BiFeO_3$[6,7] is an example of a material which is known in the two aforementioned fields. It exhibits bipolar resistive switching[8,9] and as a multiferroic material, it possesses ferroelectric DWs. It was shown that electrical properties of DWs in $BiFeO_3$ differ from those of bulk material.[10,11]

This work investigates the resistive switching properties of polycrystalline hexagonal $YMnO_3$ which has been reported as an improper multiferroic with $T_N \approx 70$ K and $T_C \approx 920$ K[12,13] and possess partially charged DWs.[14–16] In $YMnO_3$ spontaneous polarization is aligned along the c-axis perpendicular to the M-O plane and it originates from tilting and distortion of MnO_5 bipyramids and displacement of Y ions.[12,17] These transitions are driven by electrostatic and geometry effects and they lead to the formation of kaleidoscopic topology of ferroelectric trimerization-polarization DWs.[17] Piezoresponse force microscopy images reveal uniaxial structure of the domains with opposite polarization which are locked to the trimerization domains around vortex cores, yielding sixfold patterns.[17,18] It was measured that in contrary to conventional ferroelectrics, in $YMnO_3$, apart from neutral DWs, there

[a]Author to whom correspondence should be addressed. Electronic mail: a.bogusz@hzdr.de

are also charged domain walls where the opposite polarizations are facing each other: the positively head to head (HH) DWs and the negatively charged tail to tail (TT) DWs.[14–16] In addition, it was shown that the density of vortex cores which are formed during a spontaneous symmetry-breaking phase transition, i.e. at T_C, depends on the cooling rate of $YMnO_3$.[18]

So far, the predominantly investigated application of $YMnO_3$ is the metal-ferroelectric-semiconductor field-effect-transistor (MFSFET),[19–21] and there are only few reports about resistive switching of both hexagonal[22] and orthorhombic[23] $YMnO_3$ thin films. In this work we analyze the unipolar resistive switching behavior of hexagonal $YMnO_3$. The observed phenomenon is discussed in terms of presence of point defects and ferroelectric charged domains in this oxide. Our research provides a new insight into understanding the resistive switching in ferroelectric materials and can help to establish new pathways for the design of novel oxide electronic devices.

II. EXPERIMENTAL

The $YMnO_3$ (YMO) films were grown by pulsed laser deposition (PLD) on commercial Pt/Ti/SiO_2/Si substrates. Ceramic, stoichiometric YMO target and a KrF excimer laser with wavelength of 248 nm were employed during the PLD process. The laser beam was focused on the target with an energy density of 2.5 J/cm^2 and a repetition rate of 3 Hz. The substrate temperature (T_s) and oxygen partial pressure (p_{O2}) during the deposition process were fixed to 800 °C and 1.8×10^{-1} mbar (sample A) and 1.8×10^{-2} mbar (sample B), respectively. The thicknesses of the grown films were 150 nm and 200 nm for sample A and B, respectively. The crystallinity and surface morphology of the as-grown films were characterized by X-ray diffraction (XRD), scanning electron microscopy (SEM), and atomic force microscopy (AFM). Gold, circular top electrodes (TE) of diameter ranging between 240 μm and 760 μm were prepared by DC magnetron sputtering at room temperature. Resistive switching properties and resistance-temperature characteristics of the films were investigated in a metal-insulator-metal (i.e. Au/YMO/Pt/Ti) configuration in a two-point probe geometry employing a Keithley 2400 source meter and a LakeShore 331 temperature controller. The bottom electrode (BE), i.e. Ti/Pt, was grounded throughout all electrical measurements.

III. RESULTS AND DISCUSSION

A. Analysis of as-grown $YMnO_3$ films

The SEM images and XRD patterns of as-grown films are presented in Figs. 1(a), 1(b) and Fig. 1(c), respectively. According to the obtained XRD data, peaks can be assigned to the polycrystalline hexagonal $YMnO_3$ phase. The SEM images reveal the differences in surface morphology of the prepared films indicating nanocrystalline structure of sample A. The roughness mean square of the film surfaces determined by AFM measurements is 18.7 nm in case of sample A and 23.0 nm in case of sample B. In order to map the local charge distribution and related conductivity of the sample surfaces, phase sensitive AFM measurements were carried out with the use of an Anfatec Level AFM. Measurements were done in a tapping mode with a conductive tip where the change of amplitude and phase shift of the AC driven cantilever is used as a feedback signal and can be assigned not only to the variation in surface morphology but also to the locally charged areas. The latter ones might attract (repulse) the probing tip what leads to the reduction (increase) of cantilever frequency observed as a negative (positive) phase shift. Note that depending on the type of majority charge carriers in $YMnO_3$ the hole-like (electron-like) carriers are depleted (accumulated) at the charged HH DWs and accumulated (depleted) at the charged TT DWs.[24] Fig. 2 presents the images obtained with phase sensitive AFM for both samples where the non-homogenous charge distribution over the film surface can be seen. Despite strong electrostatic background force (possibly dominating the Van der Waals interactions) between the tip and sample observed during the measurement, presence of ferroelectric domains and DWs has not been revealed. The main charge accumulation regions are located at the grain boundaries. In addition, in case of sample B, local depletion regions can be recognized (clearly visible dark spots in Fig. 2(d)).

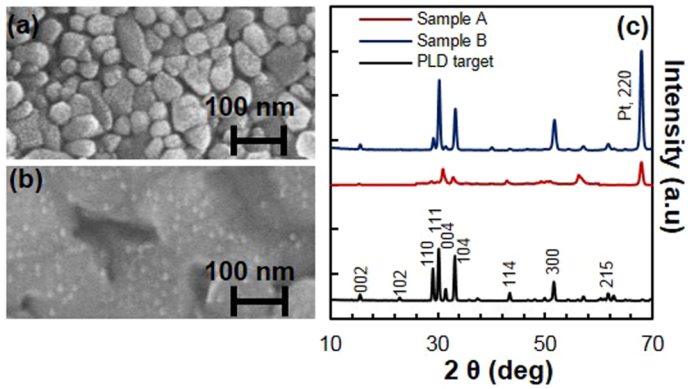

FIG. 1. SEM images of sample A (a) and B (b) and XRD patterns (c) of both as-grown films and of a ceramic $YMnO_3$ target. Obtained XRD peaks are assigned to hexagonal $YMnO_3$ phase and are labeled with Miller indices according to the International Centre for Diffraction Data (JCPDF 25-1079).

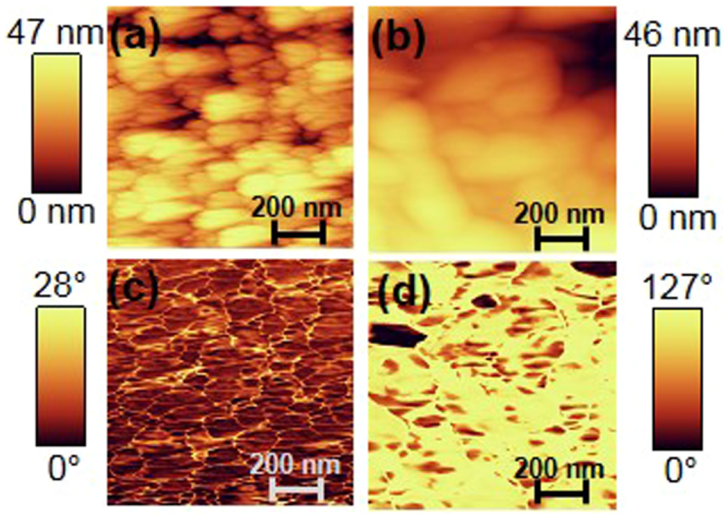

FIG. 2. Phase sensitive AFM images of sample A (a, c) and B (b, d) presenting surface topography (a, b) and respective phase shift (c, d). The contrast observed in the phase shift images corresponds to the surface charge accumulation regions which might be recognized as a grain boundaries. For sample B, also the local depletion regions, appearing as a dark areas in (d), are distinguishable within separated crystallites.

B. Resistive switching

The current-voltage (I-V) characteristics obtained in the electrical measurements reveal resistive switching in both samples as presented in Fig. 3. The set process, defined as the transition from the high resistance state (HRS) to the low resistance state (LRS) occurs at voltages, V_{SET}, 10 V and higher, while the reverse process, i.e. reset (defined as a transition from LRS to HRS) is triggered at smaller voltages, V_{RESET}. In both cases switching is abrupt (on a time scale limited by the time resolution of our set-up, i.e. 0.1 s) and is independent of the bias polarity. The latter one classifies the mode of switching as a unipolar resistive switching, commonly ascribed to the formation and rupture of conductive paths, so-called filaments, within the insulating/semiconducting layer. High current which assists the reset process (generally higher than 0.1 A) implies a significant release of Joule heating. The latter has been proposed to be the cause of rupture of the conductive filament at its weakest point.[1,2,25–27] The relation between the current in both HRS and LRS and the contact surface area is presented in the insets of Figs. 3(a), 3(b). For sample A, the current in HRS increases for larger contact areas while in LRS it stays independent of the pad size. In case of sample B, both HRS and LRS seem to be independent of the contact area. Independency of resistance values with respect to the

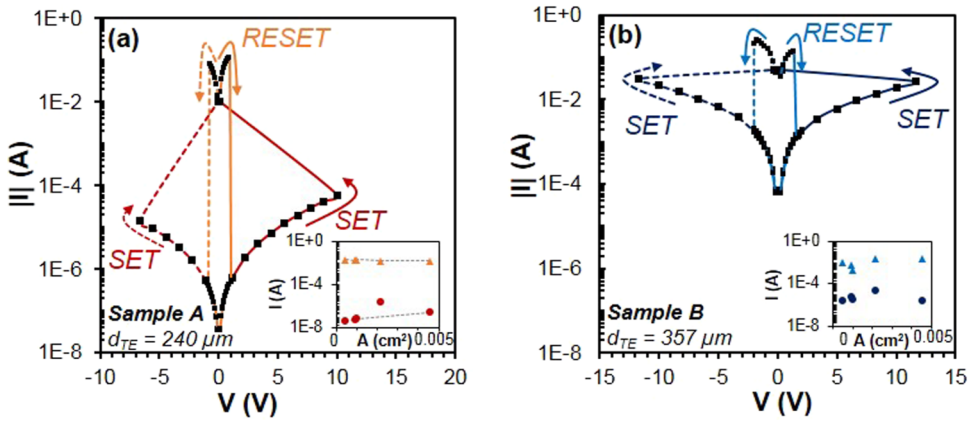

FIG. 3. I-V characteristics of sample A (a) and B (b) revealing unipolar resistive switching. Solid and dotted lines correspond to the switching events under application of positive and negative bias, respectively. The insets show the relation between the current and contact area A in LRS (triangles) and in HRS (circles). For better comparison, scale of y axis is the same for both graphs and insets.

pad size indicates that the switching is a local phenomenon.[28] These results supports the filamentary nature of observed unipolar resistive switching.[1,29] Increase of resistance in HRS with decrease of pad size points towards interface and/or bulk limited conductivity[30] in case of sample A.

Further electrical measurements confirm that both resistance states are nonvolatile, i.e. once the sample is switched into the desired LRS or HRS it stays in this state after switching off the applied electric field. Results of retention tests for both samples indicate very good stability of the HRS and LRS with the memory window between the OFF and ON state remaining constant over 14 hours. The ratio of the resistance in the HRS and LRS is approx. 10^5 and 10^3 for sample A and B, respectively. Endurance measurements indicate that the switching behavior of sample A is more stable regarding repeatability and reliability with well-defined ON and OFF states. In case of sample B, uncontrolled intermediate levels of resistance are observed. For both samples endurance is limited (below 50 cycles), most likely due to the observed damage of the top electrode. The set process, i.e. formation of conductive filaments, occurs generally at higher values of applied bias in case of the thicker sample B (200 nm). The reset process, i.e. rupture of filaments, is taking place at similar values of V_{RESET} for both samples, suggesting that it is related to the nature of the conductive path (e.g. its diameter) rather than to the thickness of the switching medium. Values of currents in the LRS do not significantly vary between both samples, remaining below 1 mA at 0.2 V while in the HRS a difference of two orders of magnitude can be observed, with sample A exhibiting smaller currents. The temperature dependence of the resistance of samples in the LRS and HRS was measured in the range between room temperature and 100 °C. The results are presented in Fig. 4. It can be seen that both samples exhibit metallic and semiconducting behavior when switched to LRS and HRS, respectively. The values of activation energy (E_a) of the low-field conduction were calculated according to Eq. (1) assuming an Arrhenius behavior:

$$R = R_0 \exp\left(\frac{E_a}{k_B T}\right), \tag{1}$$

where R_0, k_B and T correspond to the pre-exponential term, Boltzmann constant and absolute temperature, respectively. The values of E_a for conduction in the HRS were determined to be 0.44 eV and 0.33 eV for sample A and B, respectively. Our results agree with previous works on $YMnO_3$ ceramics measured up to approx. 200 °C where E_a was found to range between 0.36 eV[32,33] and 0.63 eV.[31] It is generally accepted that $YMnO_3$ exhibits p-type conductivity due to the hopping of positive holes from site to site among the localized levels at Mn^{3+} - Mn^{4+} (small polaron hopping)[31–34] and the values of E_a correspond to the activation energy of this process.

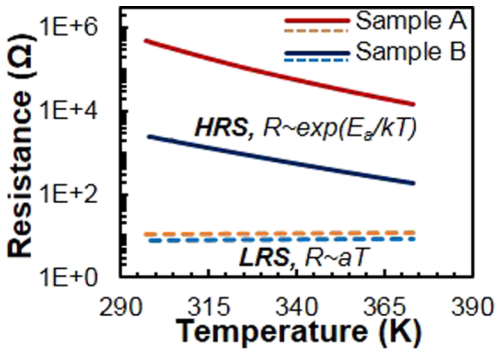

FIG. 4. Temperature dependence of resistance of sample A (black) and sample B (gray) in HRS (solid lines) and LRS (dotted lines). The diameter of TEs used for the measurement was 760 μm.

C. Contribution of the grain boundaries and charged domain walls

It can be concluded that the unipolar resistive switching observed in Au/$YMnO_3$/Pt/Ti structures is of filamentary nature. Formation and rupture of metallic filaments within the oxide layer are triggered by applied high voltage and release of Joule heating, respectively. Our conclusions are in very good agreement with work on unipolar resistive switching in $YMn_{1-\delta}O_3$ thin films.[22] There, formation of filaments localized at the defects induced by Mn vacancies was induced by the soft breakdown process in high electric field. Their rupture was assigned to the local redox reaction of Mn^{4+} to Mn^{3+} due to remarkable Joule heating. This explanation, however feasible and correct, seems to be general and does not cover extensive discussion of impact of point defects and ferroelectric properties of $YMnO_3$ into the RS. Here we discuss in further detail the possible origin of the unipolar resistive switching in multiferroic $YMnO_3$ supporting our discussion with results obtained on sample grown at lower p_{O2} and therefore with altered concentration of point defects. Results presented in this work indicate the high importance of p_{O2} during the PLD growth of $YMnO_3$ films. In addition to different switching properties, surface morphology and thickness of deposited films, also the difference in chemical composition of oxide is expected. Growth of $YMnO_3$ at high temperature results in loss of the oxygen and formation of oxygen vacancies with higher concentration for more reducing conditions. During the cooling down process, $YMnO_3$ films absorb the oxygen from atmosphere what leads to the annihilation of oxygen vacancies, according to model reaction expressed in Kröger-Vink notation by the Eq. (2):

$$V_O^{\bullet\bullet} + 1/2O_2 \Leftrightarrow O_O^x + 2h^{\bullet} \tag{2}$$

where $V_O^{\bullet\bullet}$, O_2, O_O^x and $h^{\bullet}$ denotes respectively a double ionized oxygen vacancy, an oxygen, a neutral oxygen ion at the oxygen lattice site and a positive hole. Simultaneously, some of the Mn^{2+} and Mn^{3+} are oxidized to Mn^{3+} and Mn^{4}+ cations, respectively. Both kinds of point defects, i.e. oxygen vacancies and Mn cation with other than +3 valence state, might contribute to the resistive switching. Oxygen vacancies and impurities are preferentially located at/near the grain boundaries.[35,36] In our work this can be seen as charge accumulation regions in Figs. 2(c), 2(d). It has been reported that the grain boundaries are a primary location of the local resistive switching in HfO_2[37] and WO_3.[38] In addition to the grain boundaries acting as charged regions, in $YMnO_3$ also a charged DWs exist.[14–16] HH and TT DWs are screened by accumulation or repulsion of the free charge carriers. This applies also to point defects and impurities distributed within the oxide. As a result of applied bias and local increase of temperature, the defects become more mobile. That suggests that at certain conditions (e.g. applied voltage, concentration of free carriers and defects) conductive filaments could form along both charged DWs and grain boundaries. These considerations stand in agreement with recently published work on multiferroic $BaTiO_3$ where the observed metallic conduction of the charged DWs is explained by the formation of degenerate quasi-two-dimensional (q2D) electron gas at HH DW.[39]

Results presented in this work explain observed unipolar RS phenomena in Au/$YMnO_3$/Pt/Ti structures however the exact composition of conductive filaments and mechanism of reset process requires further, in-depth analyses.

IV. CONCLUSIONS

This work presents the unipolar resistive switching characteristics of $YMnO_3$ thin films grown by pulsed laser deposition. The resistive switching is ascribed to the formation and rupture of conductive filaments preferentially located along the grain boundaries or charged domain walls. The presence of the latter ones has been discussed in terms of possible contribution into the resistive switching phenomena and the transport properties of (multi)ferroic materials. A high ratio of the resistance in the OFF and ON state and very good retention properties suggests that $YMnO_3$ is a promising candidate for resistive switching nano devices. It is proposed that engineering of domain walls and point defects could enable better control over resistive switching. This in turn might contribute to the development and design of novel resistive switching oxide electronics.

ACKNOWLEDGMENTS

The authors acknowledge the financial support from the Initiative and Networking Fund of the Helmholtz Association (VH-VI-422), China Scholarship Council (201206970006), Sächsische Aufbaubank (SAB-59948/245), and from Deutsche Forschungsgemeinschaft (DFG SCHM1663/4-1 and BU 2956/1).

[1] R. Waser and M. Aono, Nature Mater. **6**, 833 (2007).
[2] R. Waser, R. Dittmann, G. Staikov, and K. Szot, Adv. Mater. **21**, 2632 (2009).
[3] D. B. Strukov and H. Kohlstedt, MRS Bulletin **37**, 108 (2012).
[4] J. Guyonnet, I. Gaponenko, S. Gariglio, and P. Paruch, Adv. Mat. **23**, 5377 (2011).
[5] E. A. Eliseev, A. N. Morozovska, G. S. Svechnikov, V. Gopalan, and V. Y. Shur, Phys. Rev. B **83**, 235313 (2011).
[6] A. K. Pradhan, K. Zhang, D. Hunter, J. B. Dadson, G. B. Loiutts, P. Bhattacharya, R. Katiyar, J. Zhang, D. J. Sellmyer, U. N. Roy, Y. Cui, and A. Burger, J. Appl. Phys. **97**, 093903 (2005).
[7] J. Lu, A. Günther, F. Schrettle, F. Mayr, S. Krohns, P. Lunkenheimer, A. Pimenov, V. D. Travkin, A. A. Mukhin, and A. Loidl, Eur. Phys. J. B **75**, 451 (2010).
[8] Y. Shuai, S. Zhou, D. Bürger, M. Helm, and H. Schmidt, J. Appl. Phys. **109**, 124117 (2011).
[9] K. Yin, M. Li, Y. Liu, C. He, F. Zhuge, B. Chen, W. Lu, X. Pan, and R. W. Li, Appl. Phys. Lett. **97**, 042101 (2010).
[10] J. Seidel, L. W. Martin, Q. He, Q. Zhan, Y. H. Chu, A. Rother, M. E. Hawkridge, P. Maksymovych, P. Yu, M. Gajek, N. Balke, S. V. Kalinin, S. Gemming, F. Wang, G. Catalan, J. F. Scott, N. A. Spaldin, J. Orenstein, and R. Ramesh, Nature Materials **8**, 229 (2009).
[11] S. Farokhipoor and B. Noheda, Phys. Rev. Lett. **107**, 127601 (2011).
[12] B. B. Van Aken, T. T. M. Palstra, A. Filippetti, and N. A. Spaldin, Nature Mater. **3**, 164 (2004).
[13] T. Choi, Y. Horibe, H. T. Yi, Y. J. Choi, W. Wu, and S.-W. Cheong, Nature Materials **9**, 253 (2010).
[14] D. Meier, J. Seidel, A. Cano, K. Delaney, Y. Kumagai, M. Mostovoy, N. A. Spaldin, R. Ramesh, and M. Fiebig, Nature Materials **11**, 284 (2012).
[15] Y. Du, X. L. Wang, D. P. Chen, S. X. Dou, Z. X. Cheng, M. Higgins, G. Wallace, and J. Y. Wang, Appl. Phys. Lett. **99**, 252107 (2011).
[16] T. Matsumoto, R. Ishikawa, T. Tohei, H. Kimura, Q. Yao, H. Zhao, X. Wang, D. Chen, Z. Cheng, N. Shibata, and Y. Ikuhara, Nano Lett. **13**, 4594 (2013).
[17] T. Jungk, Á. Hoffmann, M. Fiebig, and E. Soergel, Appl. Phys. Lett. **97**, 012904 (2010).
[18] S. M. Griffin, M. Lilienblum, K. T. Delaney, Y. Kumagai, M. Fiebig, and N. A. Spaldin, Phys. Rev. X **2**, 041022 (2012).
[19] S. Parashar, A. R. Raju, C. N. R. Rao, P. Victor, and S. B. Krupanidhi, J. Phys. D: Appl. Phys. **36**, 2134 (2003).
[20] D. Ito, N. Fujimura, T. Yoshimura, and T. Ito, J. Appl. Phys. **93**, 5563 (2003).
[21] K. Haratake, N. Shigemitsu, M. Nishijima, T. Yoshimura, and N. Fujimura, Jap. J. App. Phys. **44**, 6977 (2005).
[22] Z. B. Yan, S. Z. Li, K. F. Wang, and J. M. Liu, Appl. Phys. Lett. **96**, 012103 (2010).
[23] Z. Chen, C. L. Ma, F. X. Wu, Y. B. Chen, J. Zhou, G. L. Yuan, Z. B. Gu, S. T. Zhang, and Y. F. Chen, Appl. Surf. Sci. **257**, 8033 (2011).
[24] W. Wu, Y. Horibe, N. Lee, S.-W. Cheong, and J. R. Guest, Phys. Rev. Lett. **108**, 077203 (2012).
[25] B. J. Choi, D. S. Jeong, S. K. Kim, C. Rohde, S. Choi, J. H. Kim, C. S. Hwang, K. Szot, R. Waser, B. Reichenberg, and S. Tiedke, J. Appl. Phys. **98**, 033715 (2005).
[26] K. M. Kim, B. J. Choi, Y. C. Shin, S. Choi, and C. S. Hwang, Appl. Phys. Lett. **91**, 012907 (2007).
[27] U. Russo, D. Ielmini, C. Cagli, and A. L. Lacaita, IEEE Trans. Electron Devices **56**, 193 (2009).
[28] A. Sawa, Mater. Today **11**, 28–36 (2008).
[29] D. S. Jeong, R. Thomas, R. S. Katiyar, J. F. Scott, H. Kohlstedt, A. Petraru, and C. S. Hwang, Rep. Prog. Phys. **75**, 076502 (2012).

[30] F. Borgatti, C. Park, A. Herpers, F. Offi, R. Egoavil, Y. Yamashita, A. Yang, M. Kobata, K. Kobayashi, J. Verbeeck, G. Panaccione, and R. Dittmann, Nanoscale **5**, 3954–3960 (2013).
[31] C. N. R. Rao, G. V. S. Rao, and B. M. Wanklyn, J. Phys. Chem. Solids **32**, 345 (1971).
[32] C. Moure, J. F. Fernandez, M. Villegas, and P. Duran, J. Eur. Ceram. Soc. **19**, 131 (1999).
[33] M. Tomczyk, P. M. Vilarinho, A. Moreira, and B. Almeida, J. Appl. Phys. **110**, 064116 (2011).
[34] P. Ren, H. Fan, and X. Wang, App. Phys. Lett. **103**, 152905 (2013).
[35] R. F. Klie and N. D. Browning, Appl. Phys. Lett. **77**, 3737 (2000).
[36] K. Watanabe, I. Sakaguchi, S. Hishita, N. Ohashi, and H. Haneda, App. Phys. Expr. **4**, 055801 (2011).
[37] M. Lanza, K. Zhang, M. Porti, M. Nafría, Z. Y. Shen, L. F. Liu, J. F. Kang, D. Gilmer, and G. Bersuker, App. Phys. Lett. **100**, 123508 (2012).
[38] D.-S. Shang, L. Shi, J.-R. Sun, and B.-G. Shen, Nanotechnology **22**, 254008 (2011).
[39] T. Sluka, A. K. Taganstev, P. Bednyakov, and N. Setter, Nat. Commun. **4**, 1808 (2013).